Dalton Transaction

ARTICLE

High temperature X-ray diffraction and thermo-gravimetrical analysis of the cubic perovskite $Ba_{0.5}Sr_{0.5}Co_{0.8}Fe_{0.2}O_{3-\delta}$ in different atmospheres

M.G. Sahini, J.R. Tolchard, K. Wiik and T. Grande[*]

$Ba_{0.5}Sr_{0.5}Co_{0.8}Fe_{0.2}O_{3-\delta}$ (BSCF) with the cubic perovskite structure is known to be metastable at low temperature in oxidizing atmosphere. Here, the thermal and chemical expansion of BSCF were studied by *in situ* high temperature powder X-ray diffraction and thermo-gravimetrical analysis (TGA) in partial pressure of oxygen ranging from inert atmosphere ($\sim10^{-4}$ bar) to 10 bar O_2. The BSCF powder, heat treated at 1000 °C and quenched to ambient prior to the analysis, was shown to oxidize in oxidizing atmosphere before thermal reduction took place. With decreasing partial pressure of oxygen the initial oxidation was suppressed and only reduction of Co/Fe and loss of oxygen were observed in inert atmosphere. The thermal expansion of BSCF in different atmospheres was determined from the thermal evolution of the cubic unit cell parameter, demonstrating that the thermal expansion of BSCF depends on the atmosphere. Chemical expansion of BSCF was also estimated based on the diffraction data and thermo-gravimetrical analysis. A hexagonal perovskite phase, coexisting with the cubic BSCF polymorph, was observed to be formed above 600 °C during heating. The phase separation leading to the formation of the hexagonal polymorph was driven by oxidation, and the unit cell of cubic BSCF was shown to decrease with increasing amount of the hexagonal phase. The hexagonal phase disappeared upon further heating, accompanied with an expansion of the unit cell of the cubic BSCF.

Introduction

$Ba_{0.5}Sr_{0.5}Fe_{0.8}Co_{0.2}O_{3-\delta}$ (BSCF) with the cubic perovskite structure has the last decade been considered as one of the most promising membrane materials for oxygen separation from air and as a cathode material for solid oxide fuel cells[1-8]. BSCF is a derivative of the cubic perovskite $SrFe_{0.8}Co_{0.2}O_{3-\delta}$ (SCF), formed by partial substitution of Sr with Ba to stabilize the cubic perovskite crystal structure while retaining a high concentration of oxygen vacancies. Since the first report on BSCF there has been a tremendous effort to study the superior transport properties and ionic conductivity of BSCF and related materials[9-10]. Low vacancy formation energy and low activation barrier for vacancy diffusion accounts for high oxygen vacancy concentration and high ionic mobility in BSCF[11]. The material exhibits very high oxygen permeation flux over a considerable temperature range.

Despite the high oxygen permeation properties of BSCF, the long term stability of the material under operation conditions is of great concern. Švarcová et al. reported that the cubic BSCF become unstable with respect to a hexagonal polymorph below 850-900 °C under oxidizing conditions[12]. The transition from the cubic to the hexagonal polymorph is quite complex, more correctly described as a phase separation involving formation of several phases[13-19]. The phase separation or structural transformation has also been observed by

compressive creep measurements[20,21], showing that cation diffusion is slowed down by formation of the hexagonal polymorph, reflecting the slow kinetics of the phase reaction below 900 °C. The creep rate of BSCF ceramics is exceptionally high, illustrating the challenge of keeping the cation diffusion low while optimizing the oxygen vacancy mobility[20]. The low creep resistance questioning the actual use of BSCF in high temperature gas separation membranes and several attempts to stabilize BSCF by chemical substitution have appeared, both to avoid the formation of the hexagonal polymorph and to increase the creep resistance[22-23].

Chemical expansion[24-25], particularly for ceria and perovskite materials with transition metals (Co, Fe) on the B–site is another concern with respect to the mechanical stability of oxygen permeation membranes[26-32]. The chemical and thermal expansion of BSCF has also been reported by several groups[33-39], showing lower chemical expansion than other similar candidate membrane materials due to smaller changes in oxygen stoichiometry and a generally larger unit cell, which is less sensitive to temperature and stoichiometry changes[38].

In this contribution we report on chemical and thermal expansivity behaviour of BSCF, conducted by *in situ* high temperature X–ray diffraction (HTXRD) and thermo-gravimetrical analysis (TGA) in various partial pressures of oxygen. The study shows that oxidation/reduction and thereby oxygen anion mobility in bulk BSCF take place at a

temperature as low as ~200 °C. Thermal expansion and chemical expansion was determined from the experimental data. Finally, the investigation provides additional information on the structural instability of cubic BSCF with respect to the hexagonal polymorph in oxidizing atmospheres.

Experimental

$Ba_{0.5}Sr_{0.5}Fe_{0.8}Co_{0.2}O_{3-\delta}$ (BSCF) powders were prepared by spray pyrolysis as described elsewhere[12]. Stoichiometric amount of Sr, Ba, Co and Fe-nitrate solutions were used as precursors to prepare the powders. The raw powder was calcined at 750 °C for 24 hours and ball milled in ethanol for 24 h, followed by heat treatment of the powder compacts at 1000 °C in air for 12 hours. The powder was finally pulled out of the furnace in order to cool the sample fast to ambient temperature to obtain the cubic BSCF polymorph and hinder the formation of the hexagonal polymorph during cooling. The particle size of the powder after heat treatment was investigated by scanning electron microscopy (SEM) using a Hitatchi S-3400N instrument.

Phase purity was determined using a Bruker AXS D8 Advance diffractometer. High temperature X-ray diffraction (HTXRD) measurements were performed using Bruker AXS D8 Advance diffractometer equipped with an MRI TCP20 high temperature camera. All the data except the 10 bar O_2 data were collected using a radiant heater with samples contained within an alumina sample holder. Data collected at 10 bar was measured using a Pt strip type resistive heater which also functioned as a sample support. A temperature interval of 25 °C and heating rate of 200 °/h were used, with data collected from 100 °C to about 1000 °C under various atmospheric conditions: 10, 1, 0.2 (air) and 0.01(1% O_2 in N_2) bar O_2, and pure N_2 (partial pressure of oxygen estimated to ~10^{-4} bar). An S-type thermocouple mounted in close proximity to the sample (~1 mm from the sample edge) was used for temperature determination using the radiant heater, while the thermocouple was welded to the Pt-strip in the high pressure setup. Patterns were collected across an angular range 15−75° 2θ, which was the 2θ range possible using the radiant heater. A step size of 0.016° 2θ was used. Total collection time per scan at one temperature was approximately 40 min. The heating rate between each temperature was 1 °C/s. The sample temperature was calibrated against separate HTXRD of a corundum standard. The unit cell parameters of BSCF were extracted via Pawley method refinement using the Bruker TOPAS software and a cubic model ($Pm\bar{3}m$) for BSCF.

Thermogravimetric measurements were conducted using Netzsch Thermal analysis system 4 (STA449). Measurements were conducted using a Al_2O_3 crucible at a heating rate of 200 °C/h from 100 °C to 1000 °C, with a dwell time of 40 minutes after every 25 °C. The time-temperature program of the TGA experiments corresponds exactly to the program used for the HTXRD experiments. Data were collected in different atmospheres: air, N_2, and O_2 in a similar way as the high temperature XRD measurements were taken. The mass changes prior to the measurement of samples were corrected for buoyancy by measurements on an empty Al_2O_3 crucible. The weight reported at each dwell temperature is the weight recorded in the end of each dwell period of 40 min.

The relative changes in the oxygen non-stoichiometry were calculated based on the TGA data, and the absolute change in the stoichiometry was estimated by using recent data for the oxygen non-stoichiometry of BSCF reported by Yaremchenko et al.[38]. The temperature dependence of the oxygen non-

stoichiometry (3-δ) was calculated by using the stoichiometry 2.53 (δ=0.47) as the oxygen non-stoichiometry of BSCF at 900 °C in air[38] as a reference point. The corresponding oxygen stoichiometry in O_2 and N_2 was estimated, assuming that the oxygen non-stoichiometry was equal for BSCF at 200 °C in all the three atmospheres used.

Results and discussion

Only reflections indexed to cubic BSCF with space group $Pm\bar{3}m$ were observed after quenching the BSCF powder in air from 1000 °C. The initial BSCF powder used in this study was therefore phase pure according to X-ray diffraction. The particle size of the BSCF was shown to be sub-micron by SEM (not shown).

Only reflections due to the cubic BSCF polymorph could be observed by HTXRD in N_2 atmosphere. Two typical patterns of the BSCF powder observed during heating in inert (N_2) atmosphere are shown in Fig. 1. The cubic unit cell of BSCF as a function of temperature, obtained by refinement, are shown in Figure 2a) together with the change in the relative weight of the BSCF powder measured in N_2. Below around 300 °C the thermal expansion of the cubic unit cell follows a linear relationship (red dotted line) with temperature. A non-linear expansion of the unit cell sets in at around 300 °C, associated with a significant mass loss. Above 400 °C the expansion of the lattice become close to linear again, accompanied with a steady mass loss.

The onset of the weight loss observed around 300 °C is due to thermal reduction of Co/Fe in BSCF, described by the heterogeneous reaction

$$Ba_{0.5}Sr_{0.5}Co_{0.8}Fe_{0.2}O_{3-\delta} = Ba_{0.5}Sr_{0.5}Co_{0.8}Fe_{0.2}O_{3-\delta'} + (\delta-\delta')/2\ O_2(g)\ (1)$$

The BSCF powder had been rapidly cooled down in air prior to HTXRD, *freezing in* a relatively high oxygen vacancy concentration since oxidation during cooling could not occur due to the fast cooling rate. During reheating in inert atmosphere the material equilibrated with the surrounding atmosphere when the oxygen anions became sufficiently mobile and the redox equilibrium (1) could take place. At around 400 °C the observed weight loss slowed down suggesting that above this temperature the BSCF materials is in equilibrium with the N_2 atmosphere within each isothermal dwell of 40 min. Below 300 °C the thermal reduction of BSCF was kinetically hindered due to the slow diffusion of oxygen anions. Between 300 and 400 °C the relaxation time for the equilibration approaches the experimental time scale, and at around 400 °C equilibrium between the oxide material and the surrounding was possible to establish within the timescale of the isothermal hold[40].

The coefficient of thermal expansion (TEC) of BSCF in N_2 below 300 °C and above 400 °C are 21.6·10^{-6} and 25.0·10^{-6} K^{-1} respectively, determined by a linear fit to the data in the temperature range 100-300 and 400-900 °C. The thermal expansion of the BSCF powders is significantly higher than values obtained by dilatometry on polycrystalline BSCF ceramics[38]. The relatively large TEC of BSCF below 300 °C is due to a spin transition[39], which is typical for Co-containing perovskites[31].

Reflections indexed to the cubic BSCF polymorph was also observed by HTXRD up to about 600 °C in pure O_2. Representative X-ray diffraction patterns collected in O_2 are shown in Fig. 1. The cubic unit cell of BSCF as a function of

temperature is shown in Figure 2b) together with the change in the relative weight of the BSCF powder measured in O_2. Initially the unit cell increases linearly with the temperature, while the weight remains constant. Between 175 and 275 °C a contraction of the unit cell is observed accompanied with a significant gain in the weight. In this temperature region the BSCF powder, quenched from high temperature in air, is oxidizing during reheating in O_2. At about 300 °C the BSCF powder becomes in equilibrium with the O_2 atmosphere during the isothermal dwell, and on further heating a close to linear expansion of the unit cell was observed accompanied by a steady weight loss due to thermal reduction of BSCF, as expressed by reaction (1).

increased before then disappearing upon further heating. A two dimensional plot of the temperature dependence of the BSCF diffraction pattern during heating in O_2 is shown in Fig. 3. The Bragg reflections due to the cubic BSCF are shifted to lower 2θ values due to thermal/chemical expansion. The onset of chemical expansion is reflected by the change in the slope around 300 °C. The two weak reflections at ~27 and ~42 (see Fig. 1, reflections marked with *) degrees 2θ are the signature of first the formation, followed by the disappearance of the hexagonal polymorph of BSCF. In the temperature region where the hexagonal polymorph was present a slight asymmetric tail of the (110) reflection of the cubic polymorph is evident due to partly overlapping reflections of the hexagonal phase.

Fig. 1 Typical Rietveld fit of the X-ray powder diffraction patterns of the BSCF powder measured at 204 and 876 °C in N_2 and 610, 715 and 876 °C in O_2. * corresponds to the two observable reflections due to the formation of hexagonal phase.

Above about 600 °C two additional weak reflections, corresponding to a hexagonal phase[12-19], appeared together with the Bragg reflections of the cubic BSCF polymorph, see Fig. 1. On further heating the intensity of the hexagonal reflections

Fig. 2 The cubic unit cell parameter of BSCF and the relative weight change of the BSCF powders as a function of temperature in a) N_2 atmosphere and b) O_2 atmosphere.

In the temperature interval where the hexagonal phase is present, an apparent contraction of the unit cell of the cubic polymorph is observed, see Fig. 2b. The phase separation resulting in the formation of the hexagonal phase is driven by oxidation, demonstrated by the diminishing weight loss in this temperature region. The reduction of the unit cell of cubic BSCF reflects a change in the composition. Based on previous reports[13-17], the reduction of the unit cell of cubic BSCF is mainly due to the formation of the hexagonal phase with high

Ba and Co-content. This means that the remaining cubic BSCF phase is enriched in Sr on A-site and Fe on B-site, which explains the contraction of the cubic unit cell mainly by the smaller ionic radii of Sr^{2+} relative to Ba^{2+}. Reduction of the Co-content on the B-site may also partly contribute to the lattice contraction since Fe has most likely a higher oxidations state than Co and thereby a smaller ionic radii.

The coefficient of thermal expansion (TEC) between 300 ºC and 600 ºC in O_2, is $28.6 \cdot 10^{-6}$ K^{-1}, in reasonable agreement with previous reports[34,35,38,39].
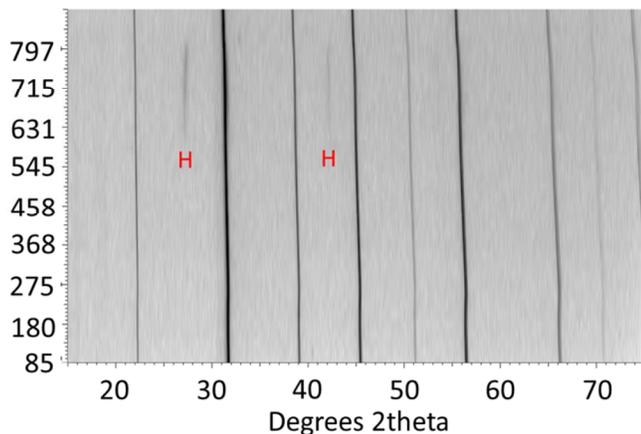
Fig. 3 2D plot of the thermal evolution of the diffraction pattern (logarithmic intensity) of BSCF powders as a function of temperature in O_2 atmosphere showing the appearance and disappearance of two reflections (H) due to the formation of a hexagonal phase. The temperature scale is not linear due to the offset in temperature from the set point temperature.

HTXRD of BSCF was also performed in three other different partial pressures of oxygen. The HTXRD data are summarized in Fig. 4a where the unit cell of the cubic BSCF is shown as function of temperature and partial pressure of O_2. Initially, thermal expansion of the unit cell is independent of the atmosphere, but above 175-200 ºC the unit cell becomes dependent on the partial pressure of oxygen. A strong contraction of the unit cell is apparent in oxidation atmospheres, and the effect was proportional to the partial pressure of oxygen as expected from eq. (1). Higher partial pressure of oxygen will shift reaction (1) to the left, reducing the oxygen non-stoichiometry (δ) and thereby lowering the unit cell volume (chemical contraction). Above approximately 300 ºC, the contraction of the unit cell at the highest partial pressure of oxygen diminished, and upon further heating a close to linear increase in the unit cell parameter with increasing temperature is evident. The unit cell is shifted upwards with decreasing partial pressure of oxygen, which clearly demonstrates the chemical expansion taking place when the partial pressure of oxygen is reduced. The apparent contraction of the unit cell above ~600 ºC, associated with the formation of a hexagonal polymorph as discussed above, is unmistakable for all atmospheres except for the data measured in N_2.

In 10 bar O_2 not only the formation of a hexagonal phase was observed. A reaction with the Pt support was detected in the same temperatures region where the hexogen phase started to appear, explaining the significant change in the unit cell parameter of cubic BSCF at this particular condition (Fig. 4a). The reaction with Pt was irreversible and pure cubic BSCF could not be obtained by further heating.

The coefficient of thermal expansion (TEC) in different atmospheres, determined by linear fit to the data in Fig 4a, is summarized in Table 1. Generally, the TEC values decrease with decreasing partial pressure of oxygen in general agreement with previous reports[33-39]. This trend reflects the suppression of the contribution of chemical expansion to the overall TEC value. The TEC values reported in Table 1 is generally higher than those reported for polycrystalline BSCF measured by dilatometry. Bulk ceramics of BSCF will not oxidize to the same extent as sub-micron powders during cooling. A lower contribution from chemical expansion due to the initial lower oxygen non-stoichiometry is therefore expected for bulk BSCF ceramics and the thermal expansion measured upon reheating will therefore be lower than for the powder.
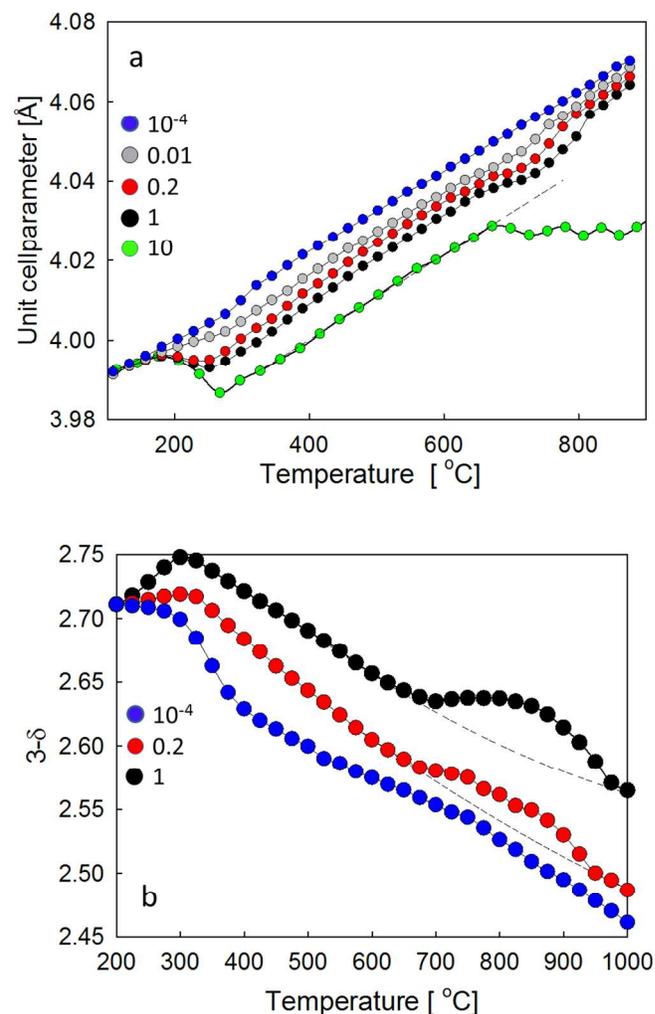
Fig. 4 a) The unit cell of cubic BSCF as a function of temperature in 10, 1, 0.2 (air), 0.01 and $10^{-4}(N_2)$ bar O_2 pressure. b) The oxygen non-stoichiometry of BSCF powder as a function of temperature in 1, 0.2 (air), and $10^{-4}(N_2)$ bar O_2 pressure.

The relative change in the oxygen non-stoichiometry of the BSCF powder was estimated from the TGA data. The absolute oxygen stoichiometry of BSCF materials has been shown to be challenging to reproduce[38], and there is still no consensus in the literature concerning the variation of the absolute oxygen non-stoichiometry as a function of temperature and partial pressure of oxygen[3,12,38,41-50]. We adapted the oxygen non-stoichiometry recently reported by Yaremchenko et al.[38] to estimate the

absolute oxygen stoichiometry of BSCF measured in pure O_2, air and N_2 as shown in Fig. 4b. Although the absolute value of the oxygen stoichiometry can be questioned, the relative change in the oxygen non-stoichiometry from 2.75 in O_2 at round 300 ºC to about 2.46 in N_2 at 1000 ºC, demonstrates the significant thermal reduction of Co/Fe in BSCF with changes in temperature and atmosphere.

Table 1 Coefficient of thermal expansion (TEC) of cubic BSCF measured by HTXRD in different atmospheres.

Temperature range [ºC]	Partial pressure O_2 [bar]	TEC [$10^{-6} \cdot K^{-1}$]
300-600	1 (O_2)	28.6
300-600	0.2 (air)	28.9
300-600	0.01	26.9
100-300	10^{-4} (N_2)	21.6
400-900	10^{-4} (N_2)	25.0

The formation of the hexagonal polymorph is associated with an apparent change in the slope of the thermal evolution of the oxygen non-stoichiometry, see Fig. 4b. This observation clearly demonstrates that the complex phase separation leading to the formation of a hexagonal phase[12-18] is driven by oxidation. The extension of the phase separation is strongly decreasing with decreasing oxygen partial pressure, both evident by the effect on the cubic unit cell and the apparent change in the oxygen non-stoichiometry. Extrapolation of the oxygen non-stoichiometry and unit cell parameter observed below the temperature region where the hexagonal polymorph is present, coincide well with the data observed in the temperature region where the hexagonal phase has vanished (see dotted line in Fig. 2b and 4b).

The chemical expansion of the unit cell at constant temperature with decreasing partial pressure of oxygen is shown in Fig. 5. A close to linear relationship between the unit cell lattice and the logarithmic partial pressure of oxygen is observed. The increasing unit cell volume with decreasing partial pressure of oxygen is a clear evidence of the chemical expansion of the lattice when the transition metal Co/Fe is reduced accompanied with an increase in the concentration of oxygen vacancies.

The chemical expansion of BSCF can be estimated from the combination of the unit cell parameters and the oxygen non-stoichiometry. The effect of chemical expansion of the lattice parameter a can be expressed through the *chemical strain* $\varepsilon_C = (a - a_o)/a_o = (\Delta a/a_o)$, where a_o is the lattice parameter in pure O_2 and a is the corresponding value in for example N_2. The *normalized chemical strain*[24] can be defined as $\varepsilon_C/\Delta\delta$ where $\Delta\delta$ is the difference in oxygen non-stoichiometry by the change in atmosphere at constant temperature. Correspondingly, the *normalized chemical expansion* can be written as $3 \varepsilon_C/\Delta\delta$. The average normalized chemical strain of BSCF (often reported as the chemical expansion coefficient), calculated by the unit cell parameter and the oxygen non-stoichiometry measured in O_2 and N_2 in the temperature range 400-600 ºC is 0.033±0.002. The chemical expansion is in excellent agreement with the chemical expansion coefficient of BSCF ceramics measured by dilatometry in the temperature range 600-950 ºC[38]. Corresponding coefficients measured by HTXRD for the related materials $La_{1-x}Sr_xCoO_{3-\delta}$[31] and $La_{1-x}Sr_xFeO_{3-\delta}$[30] are in reasonable agreement with the values for BSCF. The chemical expansion of BSCF is lower than for other alternative membrane materials, which was explained by

Yaremchenko et al. [38] by the relative large unit cell of BSCF being less sensitive to changes in oxygen non-stoichiometry.

The chemical contraction due to oxidation takes place at temperatures as low as 175-200 ºC in BSCF, see Fig 4 and 2. This demonstrates the superior oxygen ion mobility in BSCF and the enormous interest in this material from a fundamental point of view. The length scale of the diffusion process in the present experiments is ½ the size of the particle size of the BSCF powder. The time scale of the isothermal measurements by HTXRD and TGA was 40 min. The correlation of the timescale (t) and the length scale (L) can be found by $tD = 4L^2$ where D is the diffusion constant[40]. The relaxation time of the redox equilibrium (1) will therefore increase with increasing thickness of BSCF. The present data demonstrate that chemical strain in a 10-20 μm thick BSCF membrane will be induced at temperatures as low as ~300 ºC, where equilibration were observed within 40 min timescale. It also worth mentioning that the onset of reduction observed in N_2 atmosphere was shifted around 100 degrees upwards relative to the onset of oxidation (Fig. 2 and 4). We propose that the kinetics of reduction relative to oxidation is slower due to some kind of oxygen vacancy ordering at a local scale. The oxidation, leading to filling of oxygen vacancies is less sensitive to oxygen vacancy ordering than the motion of oxygen vacancy, if the oxygen vacancy ordering has occurred. The X-ray diffraction data did not provide any evidence for oxygen vacancy ordering. However, the oxygen stoichiometry become closer to 2.5 in N_2 atmosphere, see Fig 4b, which is the oxygen stoichiometry favouring oxygen ordering in perovskite oxides. The relative weight change observed during the isothermal dwell did also indicate that kinetics of equilibration was lower in N_2 atmosphere relative to the data observed in air/O_2. Particularly, an apparent increase in the relaxation time was observed in the temperature region ~600-800 ºC in N_2 (not shown). In this region the oxygen non-stoichiometry is close to 2.5 and oxygen vacancy ordering is more likely to occur.
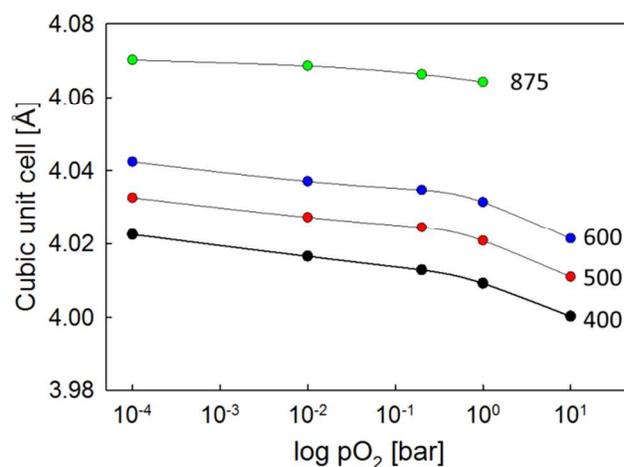
Fig. 5 The unit cell of cubic BSCF as a function of logarithm of the partial pressure of oxygen at constant temperature (ºC).

Finally, we discuss briefly the kinetics and thermodynamics of the formation of the hexagonal phase due to a phase separation process. There has been a large effort to understand the mechanism of the complex phase separation, but in most cases this has been performed on polycrystalline ceramics and often by going from high to low temperature. To the best of our knowledge this is the first study of the low temperature kinetic limit for the onset of the phase separation. Within the timescale of the experiments, it is demonstrated that the formation of the

hexagonal polymorph is initiated at temperatures as low as ~600-650 °C. The kinetics of this phase transformation is controlled by cation diffusion since diffusion has to be involved and cations are the slowest moving species. So far the compressive creep rate of BSCF is the only report related to the cation mobility[21,21]. The creep rate of BSCF is exceptionally high pointing to high cation mobility in BSCF relative to other oxygen ion conductors. The molar volume of BSCF is large and the oxygen vacancy concentration is high, and both these two phenomena, which are also related, may reduce the activation barrier for cation motion. The formation of the hexagonal BSCF is most likely limited by diffusion of A-cations since B-cations are reported to be significantly more mobile in related $LaMO_3$ materials[51-53]. The hexagonal polymorph was not observed to be formed in N_2 and the disappearance of the hexagonal polymorph was shifted to higher temperature in pure O_2 relative to air and 0.01 bar O_2 (see Fig 2a). These observations demonstrate that the phase transformation to the hexagonal polymorph is strongly dependent on the partial pressure of oxygen, and that cubic BSCF only become metastable with respect to the hexagonal polymorph at oxidizing conditions.

Conclusions

The thermal evolution of the unit cell and oxygen non-stoichiometry of cubic BSCF were determined as a function of temperature and partial pressure of oxygen. Oxidation/-reduction of BSCF was already observed to occur at temperature as low as ~200 °C. The lattice parameter is clearly dependent on both temperature and partial pressure of oxygen reflecting the significant thermal and chemical expansion of BSCF. The oxygen non-stoichiometry varied from 2.75 at ~300 °C in pure O_2 to about 2.45 in N_2 at 1000 °C. The thermal expansion coefficient of BSCF was determined in different atmospheres as well as the chemical expansion. The formation of hexagonal phase in BSCF was observed around 600 °C in oxygen and air, and the phase separation was driven by oxidation. The formation of the hexagonal polymorph reduced the unit cell of the cubic BSCF reflecting the change in chemical composition due to the precipitation of the hexagonal phase.

Acknowledgements

Notes and references

^a Department of Materials Science and Engineering, Norwegian University of Science and Technology, NO-7491 Trondheim, Norway. E-mail: grande@ntnu.no.

1   Z. Shao, W. Yang, Y. Cong, H. Dong, J. Tong and G. Xiong, *J. Membr. Sci.,* 2000, **172**, 177.

2   S. Liu, X. Tan, Z. Shao and J.D.C. da Costa, *AIChE J*., 2006, **52**, 3452.

3   P. Zeng, Z. Chen, W. Zhou, H. Gu, Z. Shao and S. Liu, *J. Membr. Sci.*, 2007, **291**, 148.

4   F.J.H. Liang, H. Luo, J. Caro and A. Feldhoff, *Chem. Mater.,* 2011, **23**, 4765.

5   A. Baumann, J.M. Serra, M.P. Lobera, S. Escolástico, F. Schulze-Küppers and W. A. Meulenberg, *J. Membr. Sci*., 2011, **377**, 198.

6   A.V. Kovalevsky, A.A. Yaremchenko, V.A. Kolotygin, A.L. Shaula, V.V. Kharton, F.M.M. Snijkers, A. Buekenhoudt, J.R. Frade and E.N. Naumovich, *J. Membr. Sci*., 2011, **380**, 68.

7   Z. Shao and S. M. Haile, *Nature,* 2004, **431**, 170.

8   W. Zhou, R. Ran and Z. Shao, *J. Power Sources*, 2009, **192**, 231.

9   J. Sunarso, S. Baumann, J.M. Serra, W.A. Meulenberg, S. Liu, Y.S. Lin and J.C.D. da Costa, *J. Membr. Sci.,* 2008, **320**, 13.

10   M. Czyperek, P. Zapp, H.J.M. Bouwmeester, M. Modigell, K. Ebert, I. Voigt, W.A. Meulenberg, L. Singheiser and D. Stover, *J. Membr. Sci.,* 2010, **359**, 149.

11   L. Wang, R. Merkle, J. Maier, T. Acartürk, and U. Starke, *Appl. Phys. Lett*., 2009, **94**, 071908.

12   S. Švarcová, K. Wiik, J. Tolchard, H.J.M. Bouwmeester and T. Grande, *Solid State Ionics,* 2008*,* **178**, 1787.

13   M. Arnold, T.M. Gesing, J. Martynczuk and A. Feldhoff, *Chem. Mater.*, 2008, 20, 5851.

14   D.N. Mueller, R.A. De Souza, T.E. Weirich, D. Roehrens, J. Mayer and M. Martin, *Phys. Chem. Chem. Phys*., 2010, **12**, 10320.

15   K. Efimov, Q. Xu and A. Feldhoff, *Chem. Mater.*, 2010, **22**, 5866.

16   P. Müller, H. Störmer, M. Meffert, L. Dieterle, C. Niedrig, S.F. Wagner, E. IversTifée and D. Gerrthsen, *Chem. Mater*., 2013, **25**, 564.

17   R. Kriegel, R. Kircheisen and J. Töpfer, *Solid State Ionics*, 2010, 181, 64.

18   J.I. Jung and D.D. Edwards, *J. Mater. Sci*., 2011, **46**, 7415.

19   F. Wang, T. Nakamura, K. Yashiro, J. Mizusaki and K. Amezawa, *Phys. Chem. Chem. Phys*., 2014, **16**, 7307.

20   J.X. Yi, H.L. Lein, T. Grande, S. Yakovlev and H.J.M. Bouwmeester, *Solid State Ionics,* 2009*,* **180**, 1564.

21   B. Rutkowski, J. Malzbender, R.W. Steinbrech, T. Beck and H.J.M. Bouwmeester, *J. Memb. Sci*., 2011, **381**, 221.

22   S. Yakovlev, C.Y. Yoo, S. Fang and H.J.M. Bouwmeester, *Appl. Phys. Lett.*, 2010, **96**, 254101.

23   S.M. Fang, C.Y. Yoo and H.J.M. Bouwmeester, *Solid State Ionics*, 2011, **195**, 1.

24   S. B. Adler, *J. Am. Ceram. Soc*., 2001, **84**, 2117.

25   A. Atkinson and T.M.G.M. Ramos, *Solid State Ionics*, 2000, **129**, 259.

26   A. Fossdal, M. Menon, I. Wærnhus, K. Wiik, M.-A. Einarsrud, and T., Grande, *J. Am. Ceram. Soc*., 2004, **87**, 1952.

27   Y. Chen and S. B. Adler, *Chem. Mater*., 2005, **17**, 4537.

28   S.R. Bishop, T.S. Stefanik and H.L. Tuller, *J. Mater. Res*., 2012, **27**, 2009.

29   D. Chen, S.R. Bishop and H.L. Tuller, *J. Electroceram*., 2012, **28**, 62.

30   X. Chen and T. Grande, *Chem. Mater*., 2013, **25**, 3296.

31   X. Chen and T. Grande, *Chem. Mater*., 2013, **25**, 927.

32   D. Marrocchelli, S.R. Bishop, H.L. Tuller and B. Yildiz, *Adv. Funct. Mater*., 2012, **22**, 1958.

33   B. Wei, Z. Lü, S. Li, Y. Liu, K. Liu and W. Su, *Electrochem. Solid State Lett*., 2005, **8**, A428.

34   Q. Zhu, T. Jin and Y. Wang, *Solid State Ionics*, 2006, **177**, 1199.

35   J. Ovenstone, J.I. Jung, J.S. White, D.D. Edwards and S.T. Misture, *J. Solid State Chem*., 2008, **181**, 576.

36 Z. Li, B. Wei, Z. Lü, Y. Zhang, K. Chen, J. Mia, W. Su,. *Ceram. Int.*, 2012, **38**, 3039.

37 M.B. Choi, S.Y. Jeon, H.N. Im, E.D. Wachsman and S.J. Song, *J. Electrochem. Soc.*, 2012, **159**, P23.

38 A.A. Yaremchenko, S. M. Mikhalev, E.S. Kravchenko and J.R. Frade, *J. Europ. Ceram. Soc.,* 2014, **34**, 703.

39. B.X. Huang, J. Malzbender, R.W. Steinbrech, L. Singheiser, *J. Membr. Sci.*, 2010, **359**, 80

40 T. Grande, J. R. Tolchard, and S. M. Selbach*, Chem. Mater.*, 2012, **24**, 338.

41 H. Wang, W. Yang, C. Tablet and J. Caro, *Diff. Fundam.*, 2005, **2**, 46.

42 S. McIntosh, J.F. Vente, W.G. Haije, D.H.A. Blank and H.J.M. Bouwmeester, *Chem. Mater.*, 2006, **18**, 2187.

43 E. Bucher, A. Egger, P. Ried, W. Sitte and P. Holtappels, *Solid State Ionics*, 2008, **179**, 1032.

44 B. Liu, Y. Zhang and L. Tang, *Int. J. Hydrogen Energy*, 2009, **34**, 435.

45 R. Kriegel, R. Kircheisen and J. Töpfer, *Solid State Ionics*, 2010, **181**, 64.

46 J.I. Jung, S.T. Misture and D.D. Edwards, *Solid State Ionics*, 2010, **181**, 1287.

47 Z. Yáng Z, A.S. Harvey, A. Infortuna, J. Schoonman, L.J. Gauckler, *J. Solid State Electrochem.*, 2011, **15**, 277.

48 D.N. Mueller, R.A. De Souza, H.I. Yoo and M. Martin, *Chem. Mater.*, 2012, **24**, 269.

49 A. Jun, S. Yoo, O. Gwon, J. Shin and G. Kim, *Electrochim Acta*, 2013, **89**, 372.

50 A.C. Tomkiewicz, M.A. Tamimi, A. Huq and S. McIntosh, *Solid State Ionics*, 2013, **253**, 27.

51 I. Wærnhus, N. Sakai, H. Yokokawa, T. Grande, M.-A. Einarsrud, K. Wiik, *Soli State Ionics*, 2004, **175**, 69.

52 J. B. Smith and T. Norby, *Solid State Ionics*, 2006, **177**, 639.

52 M. Palcut, K. Wiik and T. Grande, *J. Phys. Chem. C*, 2007, **111**, 813.

53 M. Palcut, K. Wiik and T. Grande, *J. Phys. Chem. B*, 2007, **111**, 2299.

54 M. Palcut, J.S. Christensen, K. Wiik, T. Grande, *Phys. Chem. Chem. Phys.*, 2008, **10**, 6544.

Graphical abstract

Unit cell and non-stoichiometry of $Ba_{0.5}Sr_{0.5}Co_{0.8}Fe_{0.2}O_{3-\delta}$ in O_2, demonstrating oxidation followed by thermal reduction and formation of a hexagonal phase.